IMMUNOLOGY

BCG vaccinations drive epigenetic changes to the human T cell receptor: Restored expression in type 1 diabetes

Hiroyuki Takahashi[1], Willem M. Kühtreiber[1], Ryan C. Keefe[1], Amanda H. Lee[1], Anna Aristarkhova[1], Hans F. Dias[1], Nathan Ng[1], Kacie J. Nelson[1], Stephanie Bien[2], Danielle Scheffey[2], Denise L. Faustman[1]*

The BCG (Bacille Calmette-Guérin) vaccine, introduced 100 years ago for tuberculosis prevention, has emerging therapeutic off-target benefits for autoimmunity. In randomized controlled trials, BCG vaccinations were shown to gradually improve two autoimmune conditions, type 1 diabetes (T1D) and multiple sclerosis. Here, we investigate the mechanisms behind the autoimmune benefits and test the hypothesis that this microbe synergy could be due to an impact on the host T cell receptor (TCR) and TCR signal strength. We show a quantitative TCR defect in T1D subjects consisting of a marked reduction in receptor density on T cells due to hypermethylation of TCR-related genes. BCG corrects this defect gradually over 3 years by demethylating hypermethylated sites on members of the TCR gene family. The TCR sequence is not modified through recombination, ruling out a qualitative defect. These findings support an underlying density defect in the TCR affecting TCR signal strength in T1D.

INTRODUCTION

Ten years of clinical trial data show that BCG (Bacille Calmette-Guérin) vaccinations confer health benefits to humans unrelated to protection from tuberculosis, the original goal of the vaccine. These off-target or heterologous health benefits span diverse human immune-mediated diseases. For example, BCG vaccinations can protect humans from a range of viral, bacterial, and parasitic infections and thus affect newborn mortality risks (*1*–*6*).

Adult BCG vaccinations can prevent and inhibit two different autoimmune diseases, multiple sclerosis and type 1 diabetes (T1D) (*7*–*13*). In autoimmune disease, the BCG vaccinations in adults take about 3 years for the full beneficial effects, suggesting a gradual stepwise change in the immune system. For multiple sclerosis, clinical BCG protection includes less disease relapses and also resolution of detectable brain pathologies (*8*, *9*). In diabetes, the BCG protection improves blood sugar levels and reduces insulin usage for up to 8 years (*11*). BCG vaccinations protect humans from bladder cancer and are associated with decreased risk of lung cancer (*14*, *15*). How can a >100-year-old vaccine composed of live *Mycobacterium bovis*, the bovine version of *Mycobacterium tuberculosis* (TB), lead to so many off-target and beneficial benefits in humans?

Research on the beneficial human host BCG microbe interactions frequently centers on the innate immune system. The innate immune system is composed of both monocytes and macrophages, and BCG vaccinations stimulate innate immunity days to weeks after the vaccinations are administered. Many forms of microbial and microbial cell wall components can stimulate innate immunity. Often, the monitoring of this response centers on altered cytokine patterns after microbe exposures (*16*). An older literature first noted host microbe interaction in plants and invertebrates. These studies observed a recall immune response for the innate immunity, and thus, there was some sort of "memory" (*17*). This was eventually tracked to the ability of certain infections in an acute fashion to chemically modify (methylation, acetylation, etc.) the histones in the promoters and enhancers of the genes.

This led to the term "innate immune training" because, before this time, it was not known that innate immune responses had memory (*18*, *19*). BCG is known to influence gene expression in monocytes at the level of histone acetyltransferases and chromatin remodeling by increasing the methylation of histone H3 (*20*).

Less evidence exists on beneficial off-target effects of BCG vaccinations on the adaptive human immune system and on gene pathways for immune responses and metabolism that correspond to the clinical improvements in autoimmune vaccinated subjects. Adaptive immunity involves B and T cells with antigen receptors that undergo somatic gene recombination, a feature unique to adaptive immunity. Published data show that BCG vaccinations induce host regulatory T (T_{reg}) cells by direct gene demethylation of signature genes for potent T_{reg} generation; this occurs over a 3-year time period (*12*). BCG vaccinations also in humans induce T cells (and monocytes) to augment aerobic glycolysis pathways and diminish energy metabolism through oxidative phosphorylation; this also occurs with increasing magnitude over a 3-year time frame (*12*, *13*). These BCG-induced changes again occur directly on the gene signaling pathways and gradually unfold over a time period that corresponds to clinical improvement, i.e., 2- to 3-year time course. BCG vaccinations also alter the off-target effects through T helper 1 (T_H1)/T_H17 response (*21*). An association between BCG stimulation of dendritic cell that then influences T cell populations has been reported (*22*).

The T cell receptor (TCR) is a membrane-bound heterodimer of two polypeptide chains, αβ or γδ. The TCR is the central protein complex that drives the immune response (*23*, *24*). Its diversity and antigen specificity are modulated in the extracellular domains consisting of constant (C), joining (J), and variable (V) segments. Hypervariable complementarity determining regions (CDRs) interact with various peptide antigen and major histocompatibility molecules (*24*, *25*). Recognition of ligands via the TCRαβ chain is transmitted into the cell through the CD3 complex (*26*). TCR/CD3 signaling attenuation contributes to the immaturity and malfunction in T cells

[1]Immunobiology Department, Massachusetts General Hospital and Harvard Medical School, Boston, MA 02129, USA. [2]Adaptive Biotechnologies, Seattle, WA 98109, USA. *Corresponding author. Email: dfaustman@mgh.harvard.edu

(*27*, *28*). Thus, efficient structural organization and signaling of TCR/CD3 underlie the development and function of T cells.

Genetic defects in the TCR and CD3 loci can lead to faulty T cell development that culminates in severe life-threatening immune disease. For example, quantitative impairments of TCRα constant (TRAC), CD3δ, and CD3ε are involved in human immunodeficiency disorders characterized by a lack of TCRαβ$^+$ T cells (*29*–*31*). Monogenetic TCR and CD3 defects are rare in human immune diseases but show the central role of the TCRs in human disease. Overall T cell maturation defects have long been associated with diverse forms of autoimmunity, suggesting an underlying defect in TCR selection (*32*–*35*). Intensive research has looked for T cell clones with specific mutant receptors or altered recombination errors that might explain autoimmunity, but such clones have so far never been identified.

Diverse bacteria under select circumstances epigenetically modify host DNA (*36*). The interaction of bacteria with their host is beneficial for long-lived bacteria or bacterial persistence (*37*). Bacteria-driven epigenetic changes to host cells mean that the host phenotype of cells changes without a corresponding change in the DNA sequences of the host. While the actual DNA nucleotide sequence is not affected, there can be changes in DNA methylation, in histone proteins associated with DNA or even bacterial modifications of the transcribed RNA, or more recently on the genes themselves in critical immune and metabolism pathways (*12*, *13*, *38*). The BCG organism has been reported to change host histone proteins such as H3K27 and thus can control DNA usage (*39*, *40*).

This study explores the hypothesis that microorganisms contained in the BCG vaccine can mold the human immune response at the level of the TCR and associated CD3 co-signaling receptor genes, not just at the level of histones. These two events appear to have very different time courses and also either restricted involvement of only the innate immune response or a broad response on the entire immune response. Because human autoimmunity is known to show discordance among identical twins, it is suspected that epigenetics could play a role in altered immunity. The rise in autoimmunity and allergies from deficient host-microbe interactions is an old epidemiology concept historically recognized as the hygiene hypothesis (*41*). We sought evidence of a microbe-driven epigenetic immune training process at the level of host TCR and CD3 genes. First, we compared autoimmune T cells from subjects with autoimmune diabetes to controls and then explore the in vivo impact of BCG vaccinations on direct methylation patterns on all 159 genes of TCR complex including 504 CpG sites. We also investigated at baseline and after BCG therapy all four genes of the CD3 co-receptor and 92 CpG methylation sites at baseline and after BCG therapy. We seek evidence of baseline autoimmune TCR defects driven by quantitative defects and their possible corrections with repeat BCG administrations.

RESULTS

Demographics

This study includes in vivo and in vitro experiments with a total of 117 T1D and nondiabetic control (NDC) participants. Details on the number of subjects in each experimental group are provided in Table 1, as well as in the figure legends.

Human hypermethylated genes in autoimmune subjects are TCR-related

Epigenetic mechanisms modulate the T cell phenotype and function (*42*). We therefore first compared the DNA methylation patterns of CD4$^+$ T cells from autoimmune diabetic subjects to those of controls (NDCs) before BCG vaccinations (baseline) using the Illumina methylation chips. Here, we calculated the overall methylation state of a gene at a given time point by first calculating the difference in β value of each CpG versus baseline and then calculating the average. Here, we refer to a gene as being hypermethylated if this overall β value difference is positive. For a hypomethylated or demethylated gene, this overall difference is negative.

In a genome-wide comparison of the average β values of T1D versus NDC, we found that from a total of 35,184 studied genes, 48 of the top 200 most hypermethylated genes were TCR-related (Fig. 1A, blue bars). In contrast, only 9 genes related to TCR were among the top 200 most hypomethylated genes (Fig. 1A, red bars). Thus, methylation levels of the TCR-related genes were heavily skewed toward hypermethylation in T1D subjects. A list of all top 200 hyper- and hypomethylated genes is provided (table S1), and all demographics are listed in Table 1.

Because many of the top 200 hyper- or hypomethylated genes in autoimmune diabetes were TCR-related at baseline (Fig. 1A), we studied the differences in methylation patterns for all TCR-related genes including the ones that are not in the top 200. Most individual TCR genes showed hypermethylation patterns. That was true especially in *TCRα* and *TCRβ* genes and, to a lesser extent, in *TCRγ* and *TCRδ* genes (Fig. 1B and fig. S1). Statistical significance in T1D as compared to NDC, especially in the J and V segments, was achieved. The bars for these are shown in blue (Fig. 1B). The results indicated that there are substantial differences in fundamental epigenetic levels in TCR of CD4$^+$ T cells of autoimmune diabetes as compared to NDC. These differences were even more pronounced when overall average differences between T1D and NDC were calculated on a per TCR segment basis. Although full statistical significance was not reached, the *P* values for the segments that came close are indicated in Fig. 1C. A heatmap of T1D versus NDC at the CpG level is shown (fig. S5A, left lane). The overall blue color indicates substantial reduced demethylation (increased methylation) in TCR-related genes from autoimmune diabetes subjects.

To test whether the methylation changes were associated with changes in protein expression, we next evaluated TCRαβ expression in CD4$^+$ T cells at the protein level by flow cytometry. The population of TCRαβ$^+$ cells was significantly reduced in T1D as compared to NDC (97.2 ± 1.6% versus 93.3 ± 4.6%, $P = 0.005$; Fig. 1D and fig. S6A). The mean fluorescent intensity (MFI) density of TCRαβ antibody in T1D was also significantly decreased compared to NDC (545.8 ± 101.4 versus 423.9 ± 74.5, $P = 0.01$; Fig. 1E and fig. S6A). We also attempted to quantify this difference using a TCR enzyme-linked immunosorbent assay (ELISA) assay, a less sensitive assay, on cell lysates. We were able to show the same trends, although the difference stopped short of statistical significance (fig. S7A). These results indicate that TCRαβ expression on T1D CD4$^+$ T cells is statistically decreased in autoimmune diabetes and associated with demethylation patterns that are correlated with lower levels of surface protein expression as measured by flow cytometry. This suggests a quantitative defect in TCR expression in T1D subjects.

BCG vaccinations demethylate human TCR genes in vivo to restore protein expression

We sought evidence that BCG might influence the epigenetics in T cells, an adaptive immune response, at the level of DNA methylation. We evaluated the methylation patterns of CD4$^+$ T cells from

Table 1. Demographics for participants in in vivo or in vitro studies. N/A, not available.

Baseline characteristics of type 1 diabetic and control subjects

Variable	T1D subjects, DNA methylation (*n* = 12)	T1D subjects, immunoSEQ (*n* = 27)	T1D subjects, RNA-seq (*n* = 12)	NDC subjects, DNA methylation (*n* = 8)	NDC subjects, RNA-seq (*n* = 5)	T1D subjects for various in vitro experiments (*n* = 40)	NDC subjects for various in vitro experiments (*n* = 29)
Age at blood donation, years	46.6 ± 3.0	45.5 ± 2.1	37.1 ± 3.2	26.3 ± 3.2	23.1 ± 0.3	39.2 ± 2.8	44.2 ± 3.0
Age of type 1 diabetes onset, years	24.7 ± 2.4	29 ± 2.0	19.4 ± 3.0	N/A	N/A	22.2 ± 2.2	N/A
Diabetes duration, years	21.9 ± 2.7	16.6 ± 1.1	17.7 ± 1.0	N/A	N/A	17.0 ± 1.7	N/A
% Female	7.7	40.7	30.8	62.5	60	42.5	44.4
DR3 and/or DR4 positive, %	61.6	59.3	N/A	N/A	N/A	N/A	N/A
Additional autoimmune disease—self, % *	23.1	40.7	15.4	N/A	N/A	30.0	N/A
Autoimmune disease in immediate family, %*	76.9	81.5	16.5	N/A	N/A	67.5	N/A
Islet autoantibodies at diagnosis, %	100	100	100	N/A	N/A	100	N/A

*Autoimmune diseases reported for self or for immediate family include ulcerative colitis, Crohn's disease, psoriasis, rheumatoid arthritis, lupus, celiac disease, fibromyalgia, Hashimoto's disease, hypothyroidism, ankylosing spondylitis, Graves' disease, and Raynaud's disease.

autoimmune diabetic patients at yearly intervals receiving BCG and observed a large number of genes that showed altered methylation patterns after BCG vaccination.

At year 1 after BCG vaccination, 90 of the top 200 most hypomethylated genes were TCR-related (Fig. 2A, red bars), while 3 CD3-related genes were also hypomethylated (Fig. 2A, red bars). At this same early time point, 12 TCR-related genes were hypermethylated and no CD3 gene was hypermethylated (Fig. 2A, blue bars). At year 2 after BCG vaccinations, there were 74 TCR-related and 3 CD3-related genes among the top 200 hypomethylated genes and 9 TCR-related genes among the top 200 hypermethylated genes. This trend persisted into year 3 as well. These results demonstrate that the suppression of various immunological functions including TCR/CD3 signaling may be associated with changes at the epigenetic level in the T1D $CD4^+$ T cells as compared to NDC (Fig. 1A), and BCG vaccination might restore these defects, especially in TCR/CD3-related genes (Fig. 2A).

We also evaluated the distribution of β value differences for all TCR-related genes at years 1 to 3 after BCG vaccinations versus baseline (Fig. 2B and table S2). Over time, the progressive shift toward negative β values (years 1 to 3, baseline) indicates that most of the changes corresponded to demethylation events of fairly β value–neutral genes from the middle of the histograms.

Next, we asked whether in vitro BCG treatment (i.e., cell culture in the presence of BCG) could result in the up-regulation of the TCRαβ expression at the protein level on $CD4^+$ T cells obtained from T1D patients. After 1 week of culture, the percentage of $TCR\alpha\beta^+$ cells among $CD4^+$ T cells was significantly increased in the BCG-treated group in both NDC and T1D (NDC, 98.2 ± 1.0% versus 99.2 ± 0.5%, $P = 0.007$; T1D, 98.3 ± 1.6% versus 99.5 ± 0.4%, $P = 0.02$; Fig. 2C and fig. S6B). The MFI, a measure of density of $TCR\alpha\beta^+$ cells, was also significantly up-regulated in the BCG-treated group compared to those of the nontreated group in both NDC and T1D (NDC, 446.9 ± 58.0 versus 571.2 ± 118.4, $P = 0.01$; T1D, 469.9 ± 121.8 versus 555.4 ± 133.9, $P = 0.01$; Fig. 2D). We also performed TCR antibody ELISA on cell lysates, and these showed the same trend (fig. S7B). These results illustrated that BCG treatment can directly up-regulate TCRαβ expressions on the $CD4^+$ T cells and correct the reduced expression in T1D, at least in vitro. The mechanism of restored TCR and CD3 expression from in vivo treatment with BCG vaccinations appears to be controlled, at least in part, by demethylation of the autoimmune diabetes overmethylation TCR genes.

At baseline, untreated naïve T1D subjects had many of the TCR genes hypermethylated as compared to NDCs (Figs. 1C and 3C). We therefore wanted to see whether this hypermethylation would normalize fully or partially after BCG treatment. To do this, we identified the genes that were significantly hypermethylated for T1D baseline versus NDC and then asked the question what happened 3 years later (fig. S9). We identified 28 TCR genes that were hypermethylated in baseline T1D versus NDC (fig. S9). By year 3 after BCG, 20 of 28 genes showed corrected methylation, and these were no longer statistically significant as compared to NDC (red significance lines). In 5 of 28 genes, there was desired directional correction but also some overcorrection (pink significance lines). In 3 of 28 genes, there was no correction, and these were still overmethylated (blue significance lines).

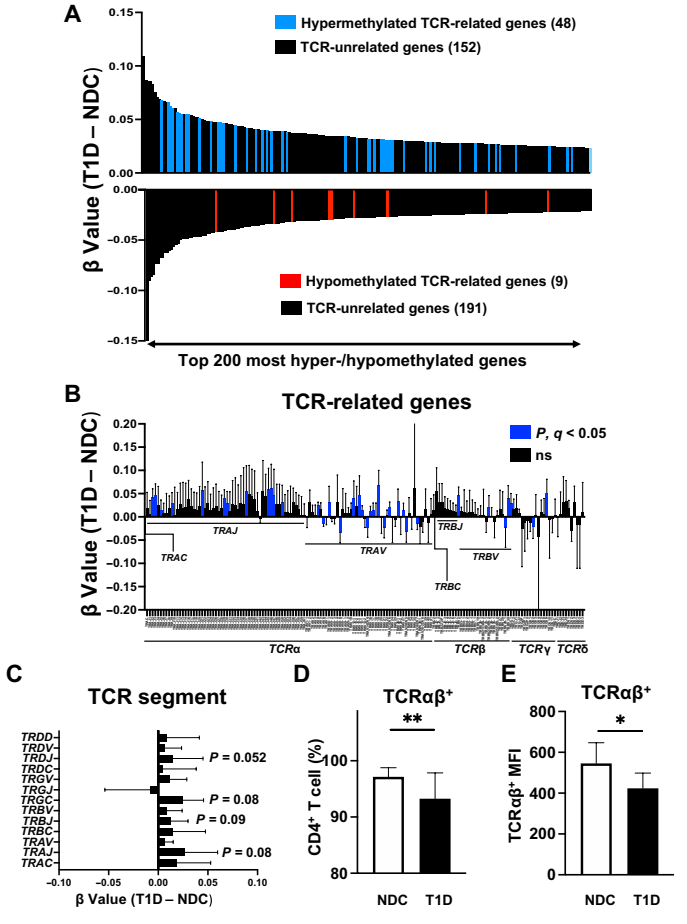

Fig. 1. TCR-related genes are hypermethylated in CD4$^+$ T cells from T1D patients as compared to NDCs. (**A**) β Values of all CpGs per gene were averaged, and the genes were ordered on the basis of the difference in average β value between T1D ($n = 12$) and NDC ($n = 8$). The figure shows the top 200 hypermethylated and top 200 hypomethylated genes among 35,184 genes in total. Forty-eight of the top 200 hypermethylated genes (24%) were TCR-related (blue bars). Among the 200 most hypomethylated genes, only 9 genes (4.5%) were TCR-related (red bars). TCR-unrelated genes are shown in black. (**B**) Differences in average β values between T1D at baseline ($n = 12$) and NDC ($n = 8$) for all TCR-related genes (average ± SD; blue bars indicate significant hypermethylation; $P < 0.05$). See fig. S1 for more details. ns, not significant. (**C**) Overall methylation in TCR segments at baseline; β values of the local region genes in C, J, V, and D segments were averaged. The differences in β values between NDC ($n = 8$) and T1D ($n = 12$) at baseline are shown for each TCR segment (average). (**D**) Analysis of the expression of TCRαβ on CD4$^+$ T cells by flow cytometry. The gating strategy for these experiments is shown in fig. S6A. The ratio of *TCR*αβ$^+$ cells among CD4$^+$ T cells in NDC ($n = 11$) and T1D ($n = 10$) is shown (average ± SD). (**E**) Mean fluorescent intensity (MFI) of allophycocyanin (APC) in *TCR*αβ$^+$ cells in NDC ($n = 11$) and T1D ($n = 10$). All statistics were Mann-Whitney *U* tests. *$P < 0.05$; **$P < 0.01$.

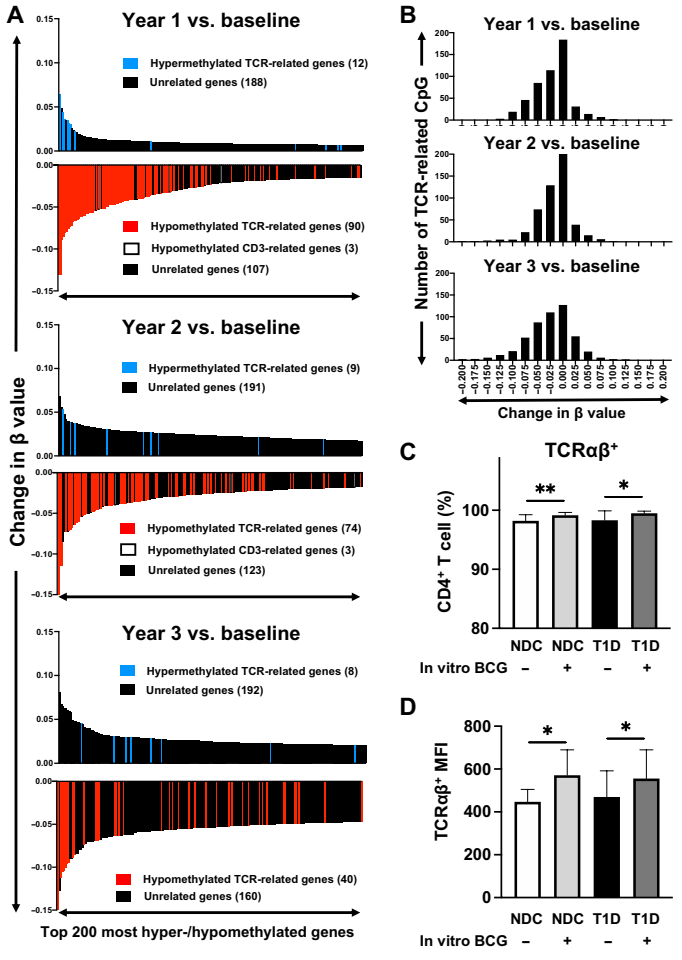

Fig. 2. Demethylation of TCR/CD3-related genes in CD4$^+$ T cells from T1D patients after vaccination with BCG. (**A**) Top 200 most hyper- and hypomethylated genes in CD4$^+$ T cells from T1D treated with BCG at baseline as compared to years 1 to 3. TCR-related genes are shown in blue (hypermethylated) or red (hypomethylated), and CD3-related genes are shown in white (hypomethylated). Unrelated genes are shown in black. Each gene and the difference in β value are shown in fig. S1A (data listed in table S1). (**B**) Distribution of β values as compared to baseline for CpGs of TCR-related genes at year 1 (top), year 2 (middle), and year 3 (bottom). A progressive shift of β values toward the left indicates progressive demethylation over time. (**C**) Changes in TCRαβ expression after 7-day culture of CD4$^+$ T cells from NDC and T1D subjects in the presence of BCG. CD4$^+$ T cells were isolated from NDC and T1D patients and cultured for 7 days in RPMI medium with or without added BCG. The cells were then analyzed by flow cytometry. The gating strategy for these experiments is shown in fig. S6B. The percentage of *TCR*αβ$^+$ cells for CD4$^+$ T cells in NDC ($n = 9$) and T1D ($n = 8$) is shown (average ± SD). (**D**) MFI of TCRαβ$^+$ cells in NDC ($n = 9$) and T1D ($n = 8$) cultured with and without BCG. All statistics were performed with two-tailed Wilcoxon testing. *$P < 0.05$; **$P < 0.01$.

This indicates that BCG had restored methylation to NDC levels for 25 of 28 TCR genes.

BCG demethylation of the host TCR occurs across most gene regions, TCRα, TCRβ, and TCRδ

In addition to analyzing TCR and CD3 presence in the top 200 hypo- and hypermethylated genes, we also evaluated the chronological changes for all TCR-related genes after BCG vaccination in more detail. Figure 3A shows the TCR-related genes individually, whereas Fig. 3B summarizes these genes by region. To assess false discovery rate (FDR), we calculated corresponding *q* values for all *P* values. The red bars in Fig. 3A indicate genes with both $P < 0.05$ and $q < 0.05$ (see table S3 for individual statistics for each gene). A more detailed view is shown in figs. S2 to S4. As was the case for the top 200 hypomethylated genes, most genes were significantly demethylated as compared to baseline at years 1 to 3 after BCG vaccination. A heatmap of these results shows the hypermethylation of the

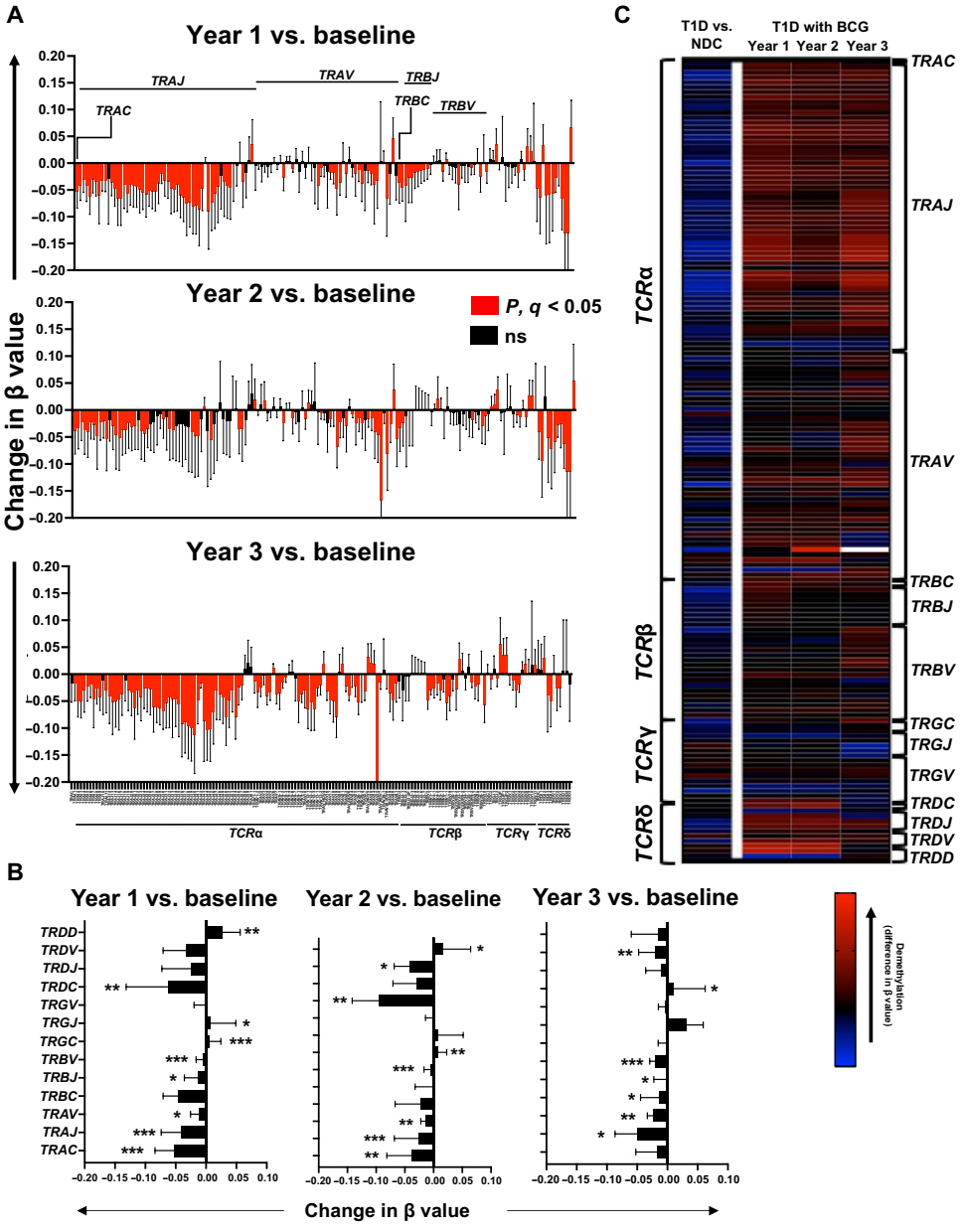

Fig. 3. The abnormally methylated TCR genes observed in T1D undergoes gradual demethylation after BCG vaccine treatment. (**A**) Chronological changes in β values of TCR-related genes from $CD4^+$ T cells of T1D ($n = 12$) after BCG vaccination as compared to baseline (year 1, top; year 2, middle; year 3, bottom) (average ± SD; red bars mean significant hypomethylation; $P < 0.05$ and $q < 0.05$, one-tailed Wilcoxon test). The graphs show progressive demethylation of the TCR after BCG vaccination over time. Figures S2 to S4 show these data in more detail. (**B**) Chronological change of average change in β values as compared to baseline in T1D ($n = 12$) at the TCR segment level after BCG vaccination (*$P < 0.05$ and $q < 0.05$; **$P < 0.01$ and $q < 0.05$; ***$P < 0.001$ and $q < 0.05$; one-tailed Wilcoxon test). All data are shown (table S2). (**C**) Heatmap of change in β values for all TCR-related genes. The left lane shows difference in β value between T1D ($n = 12$) and NDC ($n = 8$), and the right three lanes show average methylation as compared to baseline (before vaccination) at years 1 to 3 ($n = 12$ vaccinated T1D). Decreased methylation is shown in shades of red, and increased methylation is shown in shades of blue.

TCR-related genes in T1D as compared to NDC as indicated by the overall blue color (Fig. 3C, left lane), whereas subsequent demethylation as compared to baseline after BCG treatment is indicated by the mostly red color (Fig. 3C, right three lanes). Methylation patterns in *TCR*αβ and *TCR*γδ at year 2 were very similar to those at year 1, suggesting that BCG vaccinations resulted in a stable epigenetic change in TCR-related genes that persist into year 2. Furthermore, this demethylation pattern in *TCR*αβ genes was mostly retained at year 3. On the other hand, the demethylation in *TCR*δ CpGs was attenuated by year 3. Last, the opposite color patterns of *TCR*γ as compared to *TCR*α and *TCR*β in the heatmap (Fig. 3C) are indicative of relative hypermethylation in *TCR*γ.

The amount and intensity of red color in *TCR*α and *TCR*β as compared to *TCR*γ in the right three columns of the heatmap (Fig. 3C)

indicate that the methylation of *TCR*γ changes in an opposite manner. A heatmap of the TCR-related genes at the CpG level is shown in fig. S5A (right three lanes). Together, these results implied that BCG vaccination affects the epigenetics of TCR-related genes, particularly of *TCR*αβ, and that this change is maintained for at least 3 years. Thus, BCG vaccination drives DNA demethylation in the human *TCR*α, *TCR*β, and *TCR*δ genes after the treatment, and methylation is relatively stable for at least 3 years.

Quantitative defects in T1D TCR mRNA expression and restoration by BCG vaccination

Using samples from diabetic humans and NDC treated with BCG vaccination and followed for 2 years, we saw a reduction of TCR mRNA expression in most TCR genes of T1D $CD4^+$ T cells at baseline as compared to those of NDC (Fig. 4A). These differences were even more pronounced when overall average differences between T1D and NDC were calculated on a per TCR segment basis (Fig. 4B). The expression of TCR-related genes was down-regulated, except for that of *TRBJ* and *TRBD*. Tracking the change in mRNA expression after BCG vaccination in vivo over time shows that, at year 1, most TCR-related genes were up-regulated as compared to those at baseline and that the up-regulation became more pronounced at year 2 (Fig. 4C). These changes were also more pronounced on a per TCR segment basis (Fig. 4D). These results mostly tracked the methylation patterns, especially in *TCR*α and *TCR*β genes before and after BCG vaccination (Figs. 1, 3, and 4). A heatmap of these results shows the reduced mRNA expression of the TCR-related genes in T1D as compared to NDC as indicated by the overall blue color (Fig. 4E, left lane), with the notable exception of TRBJ that shows mostly increased mRNA expression (red color). Subsequent up-regulation as compared to baseline after BCG treatment is indicated by the mostly red color (Fig. 4E, right three lanes). Together, these results suggested that mRNA expression of TCR-related genes in T1D $CD4^+$ T cells was reduced at baseline and that this defect was corrected.

BCG vaccinations influence phenotypic expressions in TCR but do not affect clonotype composition of the TCRαβ repertoire

We have shown that BCG vaccination can up-regulate the expression (density) of TCR- and CD3-related genes in T1D $CD4^+$ T cells by means of epigenetic modifications that are associated with increases in both mRNA and protein levels. Furthermore, we have shown that this is associated with an attenuation in the quantitative TCR defects observed in autoimmunity across *TRAJ*, *TRAV*, and *TRBV* genes. These BCG-mediated effects were observed as early as 1 year after the vaccination and continued to be mostly present 3 years after the vaccination. All the BCG vaccination effects in the TCRαβ receptor described above were quantitative changes to phenotypic expression.

We next explored whether BCG also induced changes to clonotypes present in the TCR repertoire by performing TCR sequencing of genomic DNA (gDNA). We explored changes in TCR diversity, gene usage, and clonal expansion by sequencing the CDR3 regions of human TCRα and TCRβ chains using the immunoSEQ Assays (Adaptive Biotechnologies, Seattle, WA). The clinical traits of the subjects in this study are available (Table 1). At year 3, we observed a trend for increasing TCRβ clonality, suggesting a focusing of the repertoire (Fig. 5), but this was not accompanied by a decrease in sample richness (Fig. 5). There was no significant increase in clonal expansion (Fig. 5D). A few significant changes in gene usage at year 3 relative to baseline were found and were limited to TCRβ (Fig. 5A). No significant changes were seen for TCRα (fig. S8). These results argue against BCG mechanism of clinical improvement being centered on BCG, altering a specific islet autoreactive T cell clone that solely causes T1D. Rather, these results suggest that BCG vaccinations alter phenotypic expressions of density for improved T cell selection and signaling. At least with this method of TCR repertoire profiling, BCG is not playing a major role in altering the frequency of particular clonotypes present in the immune repertoire of TCRαβ T cells. Our results suggest that, while BCG vaccinations alter phenotypic expressions, they do not alter the frequency of particular clonotypes present in the immune repertoire of TCRαβ T cells.

The CD3 chains associated with the TCR are hypermethylated at baseline in autoimmunity

Having demonstrated consistent quantitative defects in DNA methylation patterns and protein levels in TCR in $CD4^+$ T cells from T1D patients, we also analyzed CD3 genes in the same manner for other defects, possibly affecting TCR activation and receptor expression. For proper TCR signaling, the multiple chains of CD3 associate with the TCR to generate the activation signal in T cells. All CD3 genes except for *CD3*ε exhibited hypermethylated patterns in T1D at baseline, although none reached significance (Fig. 6A). A heatmap of *CD3* methylation at the CpG level is shown (fig. S5B, left lane). As expected in the case of hypermethylation, RNA sequencing (RNA-seq) analysis showed the same trend and showed that the mRNA expressions of *CD3*γ, *CD3*δ, *CD3*ε, and *CD3*ζ were all reduced in autoimmune diabetes at baseline (Fig. 6B and table S4; note that the data did not reach significance). We also quantified the protein expression levels using flow cytometry and saw that the percentage $CD3^+$ T cells in the $CD4^+$ T cell population was reduced in T1D as compared to NDC at baseline (96.7 ± 1.8% versus 92.9 ± 6.2%, $P = 0.04$; Fig. 6C). The MFI of $CD3^+$ T cells in T1D was significantly decreased as compared to those in NDC (1393.2 ± 107.2 versus 1237.9 ± 135.6, $P = 0.02$; Fig. 6D). Protein levels as measured by ELISA to evaluate CD3 subunit levels supported the underlying quantitative defects in T1D of lowered expression, which could be controlled by hypermethylation (fig. S7C).

BCG vaccinations demethylate the CD3 gene subunits and restore mRNA expression

Having shown that CD3 is hypermethylated and that CD3 mRNA expression is reduced in $CD4^+$ T cells from T1D subjects, we next asked whether or not BCG vaccination could correct the CD3 gene methylation pattern and restore protein levels.

All subunits of the CD3 gene were demethylated at 1 year after BCG vaccination as compared to baseline (Fig. 7, A and B). This demethylation pattern persisted in the subsequent 2 years except for *CD3*ζ that became slightly hypermethylated at year 3. This tendency is supported by the distribution of β value differences for all CD3 CpGs at years 1 to 3 versus baseline (Fig. 7E and table S2). The CD3 mRNA expression over time was also consistent with the methylation patterns. After the BCG vaccinations, the expression of all CD3 genes was all increased during all 3 years (Fig. 7, C and D). Figure S5B shows a heatmap of these results at the CpG level (right three lanes).

We also wanted to see whether these same in vivo BCG effects could be observed in vitro. After in vitro culture with BCG for 7 days, the percentage of $CD3^+$ cells among $CD4^+$ T cells was significantly

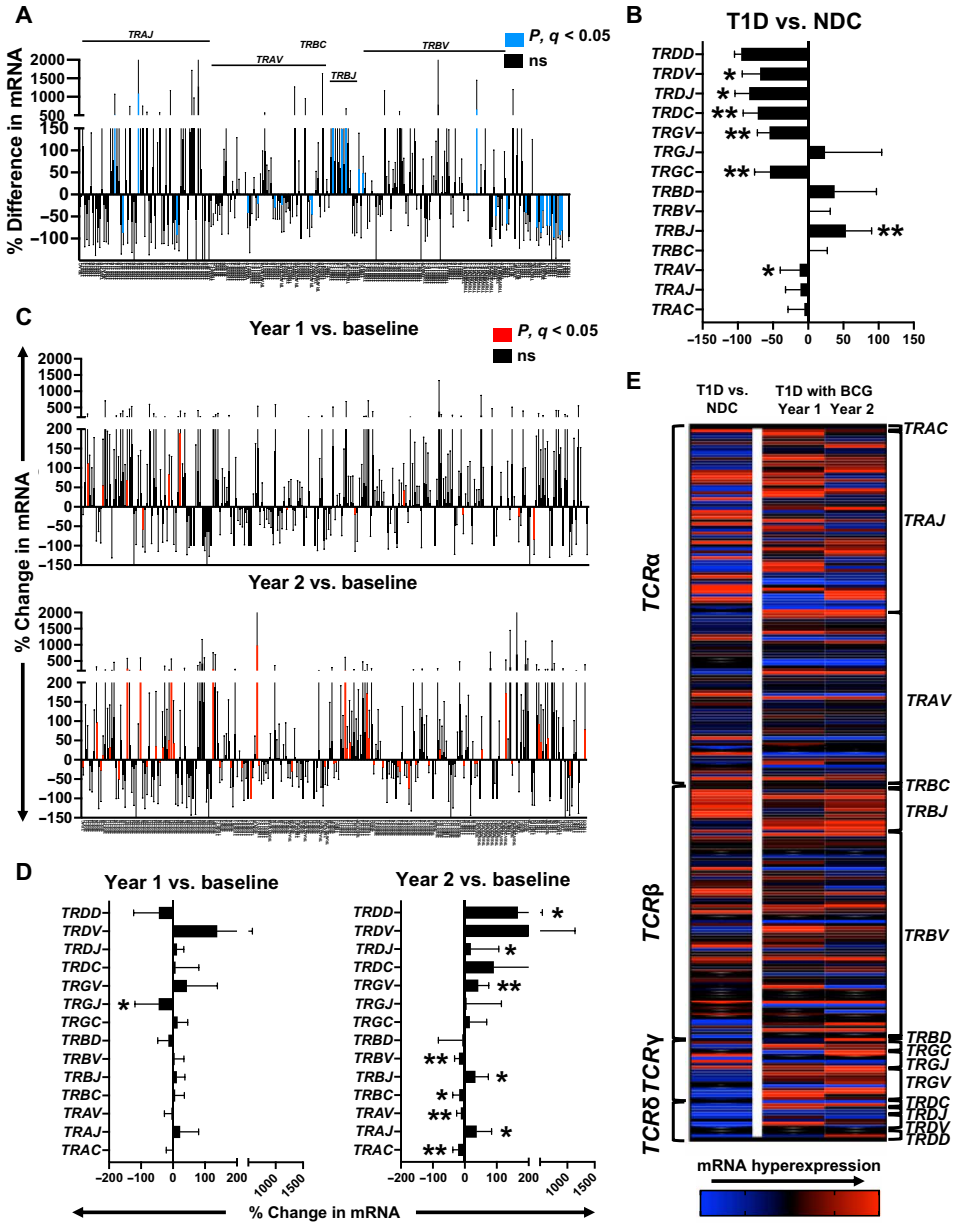

Fig. 4. Comparison of mRNA expression from CD4$^+$ T cells of T1D and NDC, and change of all TCR gene expression after BCG vaccination using RNA-seq. (**A**) Relative difference (%) in mRNA expressions in NDC ($n = 4$) and T1D ($n = 10$) CD4$^+$ T cells at baseline for all TCR-related genes (average ± SD; blue bars indicate significantly decreased expressions with $P < 0.05$ and $q < 0.05$; one-tailed Mann-Whitney U test). (**B**) Overall relative difference in mRNA expression of TCR segments at baseline; mRNA expression of the local region genes in C, J, V, and D segments was averaged. The percent differences in mRNA expression between NDC ($n = 5$) and T1D ($n = 10$) at baseline (T1D/NDC) are shown at each TCR segment (average, *$P < 0.05$ and $q < 0.05$; **$P < 0.01$ and $q < 0.05$; one-tailed Mann-Whitney U test). (**C**) Chronological changes in mRNA expression of TCR genes from CD4$^+$ T cells of T1D ($n = 9$) after BCG vaccination as compared to baseline (year 1, top; year 2, bottom) (average ± SD; red bars mean significantly increased expressions; $P < 0.05$ and $q < 0.05$; one-tailed Wilcoxon test). (**D**) Chronological change of average change in mRNA expression as compared to baseline in T1D ($n = 9$) at the TCR segment level after BCG vaccination (*$P < 0.05$; **$P < 0.01$; one-tailed Wilcoxon test). (**E**) Heatmap of change in mRNA expression for all TCR-related genes. The left lane shows difference in mRNA expression between T1D ($n = 4$) and NDC ($n = 4$), and the right three lanes show the average mRNA expression as compared to baseline (before vaccination) at years 1 and 2 ($n = 9$ vaccinated T1D). Shifts to increased expression are displayed in shades of red, and shifts to reduced expression are displayed in shades of blue.

increased in the BCG-treated group as compared to the nontreated control group in both NDC and T1D (NDC, 99.3 ± 0.4% versus 99.6 ± 0.3%, $P = 0.03$; T1D, 99.3 ± 0.4% versus 99.8 ± 0.2%, $P = 0.01$; Fig. 7E). The density of protein measured through the MFI of CD3$^+$ on T cells was also significantly higher in the BCG-treated group as compared to the nontreated group in both NDC and T1D (NDC, 1279.1 ± 182.7 versus 1560.8 ± 219.9, $P = 0.005$; T1D, 1312.9 ± 246.1 versus 1509.1 ± 220.1, $P = 0.02$; Fig. 7F). ELISA results also showed the same trend of up-regulation of protein levels by BCG treatment in culture, although the flow cytometry measurements of CD3 density

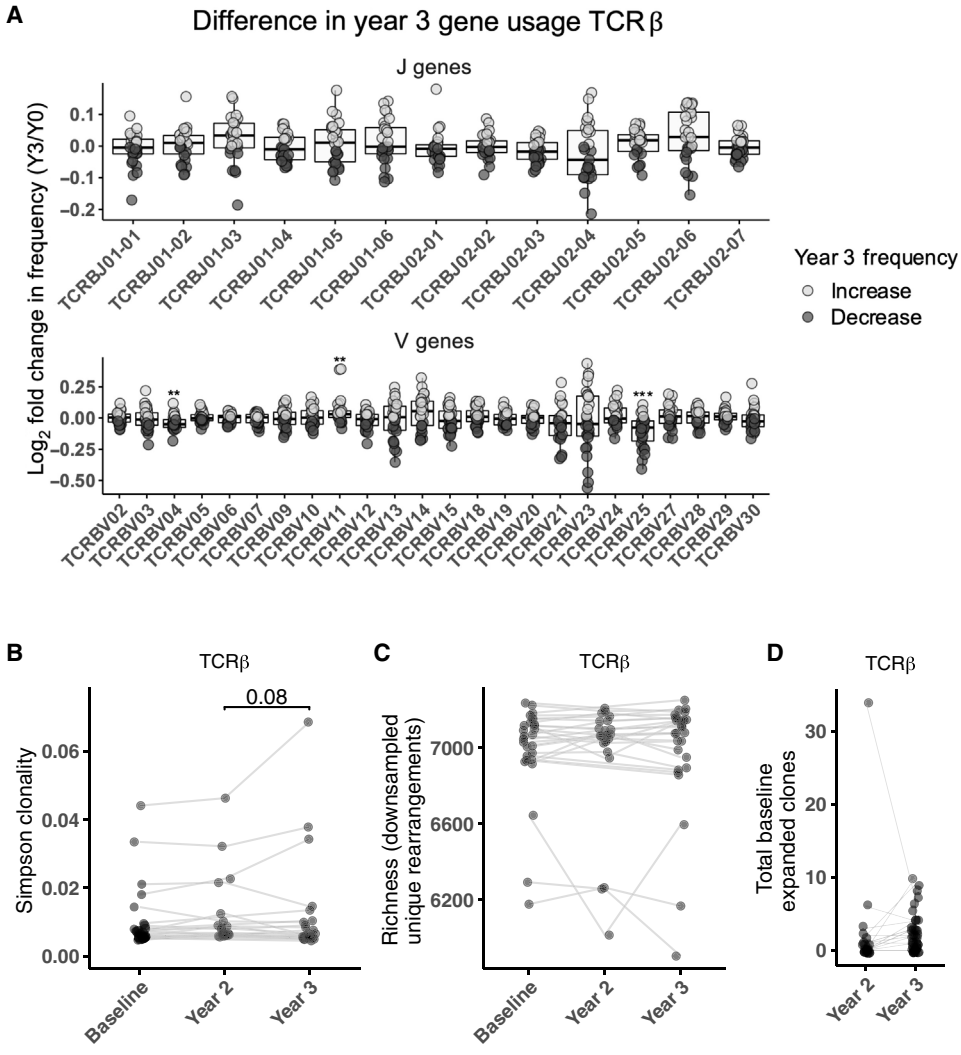

Fig. 5. BCG vaccinations are not associated with clonotype expansion, changes in gene usage, or diversity of TCRB in the T1D CD4$^+$ T cell repertoire. (**A**) Fold change of TRBJ and TRBV gene usages in peripheral CD4$^+$ T cells from patients with T1D ($n = 27$). Each point represents a change in gene usage from baseline to year 3 for a given patient. Light and dark gray coloring of points corresponds to increasing and decreasing usage, respectively. Significant changes in usage shown; Benjamini-Hochberg adjusted P from one-sample Wilcoxon with $\mu = 0$, *$P < 0.05$; **$P < 0.005$; ***$P < 0.0005$. (**B** to **D**) Simpson clonalities, downsampled richness, and count of baseline expanded rearrangements shown for TCRβ; P from Wilcoxon signed-rank test. Lines connect longitudinal samples from the same subject.

were more statistically significant (fig. S7D). Together, these results demonstrate that epigenetic and protein expression defects in CD3 from epigenetics to protein expression in T1D are correlated with BCG treatment as studied at the gene, mRNA, and protein levels. These observations of BCG-mediated systemic effects in CD3 on autoimmune diabetes mirror the effects described above for the TCR.

Up-regulated TCR/CD3 expression by BCG results in restored signaling through multiple kinases

For evaluating the change of kinase activity in TCR/CD3 signaling pathway by BCG vaccination, we performed a protein array with CD4$^+$ T cell lysate. The results show that not only well-known TCR signal pathway–related kinases such as extracellular signal–regulated kinase 1/2 (ERK1/2), p38 mitogen-activated protein kinase (MAPK), and signal transducer and activator of transcription (STAT) but also c-Jun, glycogen synthase kinase–3α/β (GSK-3α/β), c-Jun N-terminal kinase (JNK), and WNK1 were phosphorylated by BCG (Fig. 7, F and G). Thus, BCG vaccination increases phosphorylation of multiple kinases in TCR signaling pathway, confirming the functional significance of these changes.

DISCUSSION

In this study, we describe the effects of BCG vaccinations on TCR/CD3 expression in the context of autoimmunity. We identify that significant quantitative defects in TCR and CD3 proteins in CD4$^+$ T cells in untreated T1D subjects both in the TCR complex genes and the associated CD3 genes were overmethylated; this correlated with down-regulated cell surface expression or density. With multidose BCG vaccine therapy, we observed that more than 23,000 genes were demethylated at the year 1 time point, and 90 of the top 200 most hypomethylated genes were TCR-related. This process was over a 3-year-long time period that correlated with past reported improvements in the disease (*12*).

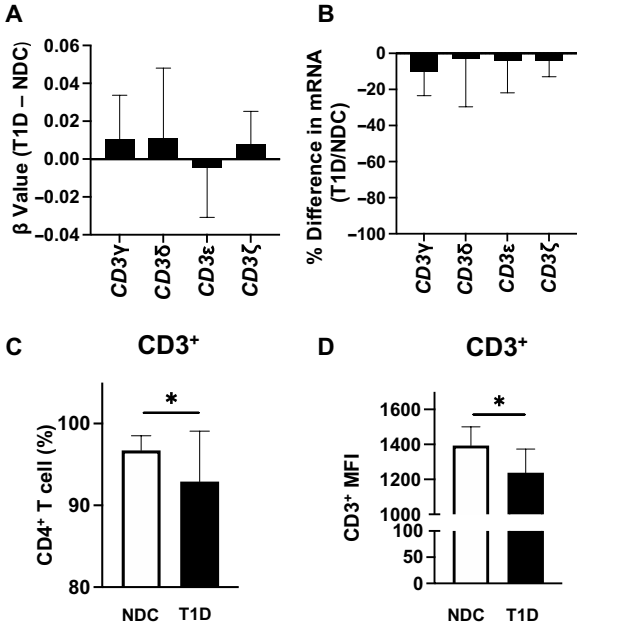

Fig. 6. Comparison of CD3 levels in CD4$^+$ T cells of T1D and NDC patients using DNA methylation, RNA-seq, and flow cytometry. (**A**) Differences in β values between NDC ($n = 8$) and T1D ($n = 12$) at baseline (T1D-NDC) for each CD3 gene (average ± SD; none of the differences were significant, one-tailed Mann-Whitney *U* test). The positive bars indicate hypermethylation in T1D, whereas the negative bars indicate hypomethylation. (**B**) Relative difference (%) in mRNA expressions of NDC ($n = 5$) and T1D ($n = 10$) CD4$^+$ T cells at baseline (average ± SD; none of the differences were significant, one-tailed Wilcoxon test). (**C**) Percentage of CD3$^+$ cells among CD4$^+$ T cells in NDC ($n = 11$) and T1D ($n = 10$) (average ± SD; *$P < 0.05$, one-tailed Mann-Whitney *U* test). (**D**) MFI of APC in CD3$^+$ cells in NDC ($n = 11$) and T1D ($n = 10$) (average ± SD; two-tailed Mann-Whitney *U* test).

Demethylation driven by BCG vaccinations is demonstrated to be stable based on over 3 years of monitoring, suggesting a durable epigenetic effect that correlated with clinical improvement, which lasts at least 8 years (*12*). We show that the BCG induced demethylation of most of the TCR-related genes and all four subunits of the CD3 complex at the level of individual gene methylation patterns by the BCG microbe and that this 3-year time period correlated with reported clinical improvements. The change in methylation patterns was associated with up-regulation of the mRNA of the same genes due to signaling being restored and a restoration of the protein levels of CD3/TCR complex. This is a human example of microbe-driven direct gene changes by a microbe, *M. bovis*, at the DNA level, affecting expression and function of the human TCR/CD3 complex. Restored function was shown in parallel kinase assays.

A goal for a significant time period in the field of immune diseases has been to identify the specific T cell clones reactive to organ-specific antigens, a process that might drive immune-mediated disease and allow specific therapy design. TCR control can also be influenced by rare point mutations associated with disease from random recombination, poor or augmented cognitive interactions with human leukocyte antigen (HLA) class I/II polymorphisms, and improper recombination events (*43*). The data here suggest an alternative defect, not necessarily exclusive, as a driver of autoimmunity and thus altered T cell selection. We suggest that this defect can be resolved by quantitative corrections to restore immune signaling. This paper identifies a major quantitative, not qualitative, defect in the TCR/CD3 protein complex and the nearly 127 genes of this complex resulting in decreased expression in T1D. This underlying defect, i.e., the surface density of the TCR, can be treated at least partly with repeat BCG vaccinations. From a basic science viewpoint, it is recognized that TCR engagement and signaling are affected by the intermolecular distance between TCR proteins and activation diminishes when proximity is increased between TCR surface proteins (*44*). Collectively, our results and the basic science data suggest that T cells are triggered by a mechanism of overall receptor proximity for intracellular signaling, now also confirmed in these studies. Spatial thresholds for TCR triggering are now identified as an underlying defect in autoimmunity, corrected by BCG as it increases TCR density after therapy to near-normal levels (*45*).

Graded knockout murine models with mutations in the TCR signaling pathway can drive different murine autoimmune disease by altering thymic T cell selections as well as regulatory T cell function (*46*–*48*). The expression density of receptors on the surface of T cells affects the type and intensity of T cell signaling responses (*49*–*53*). The data here support the concept of the regulation of T cell signaling in T1D by quantitative changes in TCR expression and not by TCR defects, resulting in a pathogenic clone. The data here did not identify a single impaired TCR that influenced disease outcome. For all autoimmune diseases, it has long been appreciated from human identical twin studies that discordance in autoimmune twins is the norm, and thus, a strong environment influence exists for autoimmune disease expression (*54*). Epigenetic relationship of genes controlled by microbes could be a candidate for this well-established disease discordance. This discordance in human identical twins with autoimmunity is more compatible with quantitative gene expression defects, not qualitative gene effects, which would not necessary be concordant between twins because their DNA should be identical. Epigenetics is known be a strong influencer of proper T cell selection among TCR affinity, TCR density, and T cell activity (*55*). Experimental murine data suggest that the TCR ligand potency and density are both contributory to the routes to T cell responses and peripheral tolerance in the induction of Foxp3 cells as well (*56*). The hypermethylation patterns were not limited to specific segments of the TCR or CD3 genes, but nearly all segments in TCR and CD3 genes were affected. Upon BCG vaccinations, regions of the TCR/CD3 complex displayed demethylation, resulting in restoration of near-normal protein levels. Because the density of TCR reflects strength of the signal (*57*), decreased MFI of TCR/CD3 on CD4$^+$ T cells argues that reduced density of the complex and abnormally short TCR length might imply the immaturity of the cells in autoimmunity. For over 20 years, it has been noted that the peripheral T cells of many autoimmune disease have a surface phenotype of immaturity, such as low levels of mature T cells expressing CD45RO (formerly known as the 4B4 protein) (*32*, *33*). This developmentally immature phenotype is a symptom of T cell immaturity linked most commonly to inadequate TCR/CD3 engagement (*33*, *34*). In addition, many human autoimmune diseases have defects in T_{reg} action, another cell population influenced by TCR density (*58*). BCG organisms can also modulate host genes such as the T_{reg} genes to restore T_{reg} potency from a baseline state of a deficiency (*59*). In many autoimmune diseases, the HLA class I complex, the reciprocal engagement complex for the TCR/CD3 complex on CD8$^+$ T cell selection, is also known in human and murine autoimmune diseases to be associated with lowered density that would potentiate poor T cell selection (*60*–*63*).

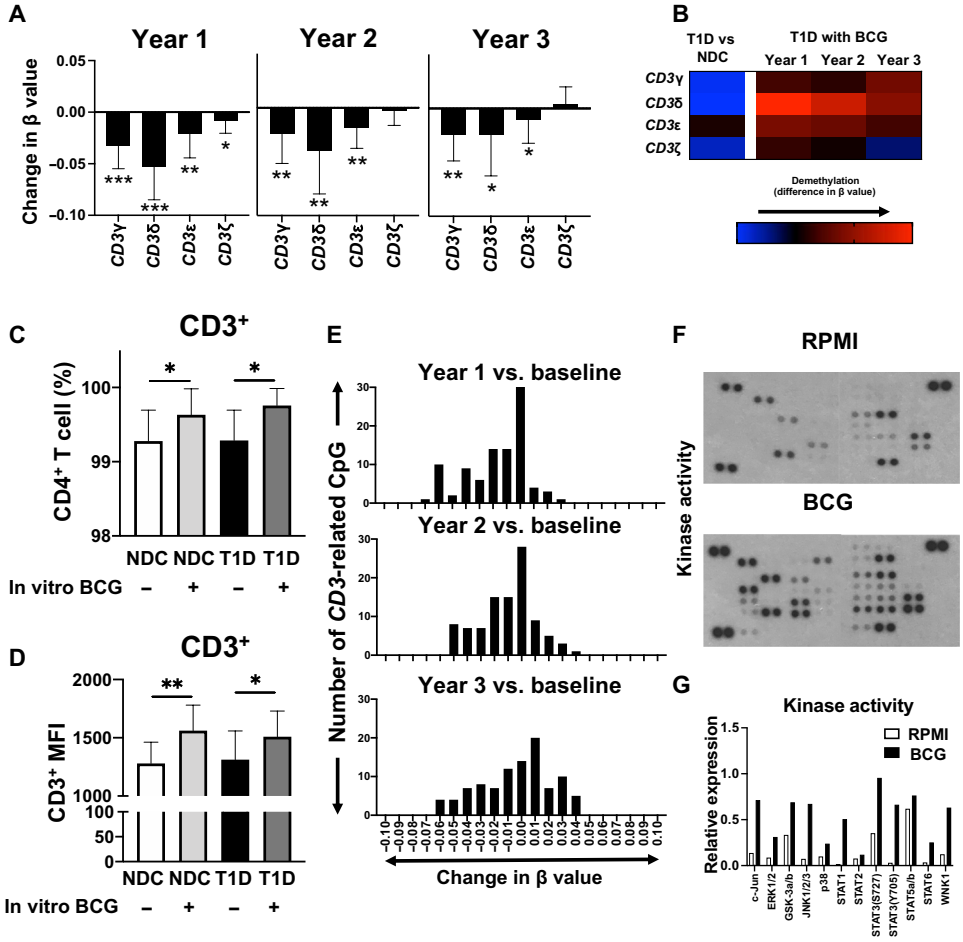

Fig. 7. Increased CD3 expression after BCG treatment in vivo and in vitro. (**A**) Change in average β values for CD3 genes in T1D ($n = 12$) as compared to baseline at 1 to 3 years after BCG vaccination (average ± SD; $^*P < 0.05$; $^{**}P < 0.01$; $^{***}P < 0.001$, one-tailed Wilcoxon test). (**B**) Heatmap indicating methylation patterns in all CD3 genes. The left lane shows difference in β value between T1D ($n = 12$) and NDC ($n = 8$), and the right three lanes show the difference in β value for T1D ($n = 12$) at baseline versus at 1 to 3 years after BCG vaccination. Hypomethylation is shown in shades of red, whereas hypermethylation is shown in shades of blue. (**C**) $CD4^+$ T cells were isolated from NDC ($n = 9$) and T1D ($n = 8$) and cultured with or without BCG for 7 days. The cells were then washed, stained for CD3, and analyzed by flow cytometry. The percentage of cells that are positive for CD3 is shown (average ± SD; $^*P < 0.05$; two-tailed Wilcoxon test). (**D**) MFI CD3 flow cytometry. The MFI for NDC ($n = 9$) and T1D ($n = 8$) cultured with or without BCG is shown (average ± SD; $^*P < 0.05$; $^{**}P < 0.01$; two-tailed Wilcoxon test). (**E**) Histograms showing the distribution of the β values as compared to baseline for CpGs of CD3-related genes at year 1 (top), year 2 (middle), and year 3 (bottom). A progressive shift of β values toward the left indicates progressive demethylation over time. (**F**) A protein array was performed to evaluate the change in some kinase in TCR signaling pathway. Upper and lower images indicate the nontreated and BCG-treated $CD4^+$ T cells, respectively. (**G**) The density of kinase in the protein array was qualified by densitometry. White and black bars indicate the values in the nontreated ($n = 1$) and BCG-treated $CD4^+$ T cells ($n = 1$), respectively.

This study extends predominantly histone modification and chromatin remodeling during bacterial infections or epigenetics of a single gene from a microbe exposure to an entire family of 163 TCR/CD3 genes involved in the immune response. This is an example of direct gene regulation, not just regulation at the level of chromatin and histones that occurs but at very early time points after the vaccines (days or weeks). Recently, the topic of epigenetics and microbe exposures through vaccinations to infectious disease has been reviewed and covered diverse human exposures beyond BCG and tuberculosis but extended to human papilloma virus, Epstein-Barr virus (EBV), hepatitis C, *Helicobacter pylori*, and more that influence single gene expression (*36*). In addition, the emerging role of epigenetics in human autoimmune disorders frequently centers on defects in microRNAs or histone posttranslational modifications, including H3K27me3 (*64*). Vaccinations and direct microbe exposures can modify the human epigenome and modulate the immune response, and histones are often modified and single genes are involved. These fundamental and BCG-driven BCG modifications of the central TCR change in the TCR are remarkable.

Limitations of the study

There are study limitations to the basic science study of these human data. We do not know whether the major changes in methylation of the TCR/CD3 receptor complex are specific to the BCG microorganisms or whether other less ancient organism also epigenetically can modify the host TCR complex.

In the human, we cannot distinguish between functionally important CpG sites in the human and CpG sites with more minor

functional roles. Therefore, these results should be revisited in the future as newer, more comprehensive methylation chips become available and when more information becomes available in the human in which CpG sites encode the pivotal functions in TCR/CD3 protein complex expression.

Our clinical trials do not allow for the treatment of NDC with BCG. Therefore, a comparison of T1D and NDC with BCG vaccinations is not possible. In addition, there is a substantial difference in average age between T1D and NDC groups, and we cannot exclude that there may be an age-associated difference in gene methylation between young and old T1D.

Here, we describe associations and correlations between treatment with BCG and longitudinal changes in gene methylation. We would like to hypothesize that there is a causative relation between the treatment and our longitudinal methylation observations and past published data on the corresponding beneficial clinical effects over the same time course. However, causation in complex biological systems is very hard to prove. The same also holds for our observations that show correlations between gene methylation changes and changes at the mRNA or protein expression level.

These freshly isolated $CD4^+$ T cells were confirmed >85% pure by flow cytometry (fig. S6E). Even with excellent cell sorting, some antigen-presenting cells including dendritic cells or macrophages might have been present. This would not affect the TCR only present on T cells but could bridge BCG recognition by $CD4^+$ T cell in vitro culture experiments. In addition, this study used these bulk $CD4^+$ T cells and subcomponents such as autoreactive cells and naïve, memory, and regulatory T cells were not distinguished. This was due to limited amount of blood sampling from one trial patient. We obtained approximately 10 million to 20 million $CD4^+$ T cells from one blood collection (20 ml), and at least 5 million cells are required for DNA, RNA extraction, and ELISA, respectively. Therefore, analyses in detailed populations and fractions from $CD4^+$ T cells were not realistic in this study. Future studies will also need to focus on $CD8^+$ T cells from subjects treated with BCG vaccinations for the impact on this T cell subpopulation as well.

MATERIALS AND METHODS

Human clinical trial study and the data

All studies with human samples had full institutional approvals in Massachusetts General Hospital and Partners Health Care (study nos. 2007P001347, 2012P002243, and 2013P002633), and the interventional studies using past BCG-treated subjects and open label–treated subjects who were also formally approved by the U.S. Food and Drug Administration (IND#2007P001347 and IND#2013P16434). All blood donors, both T1D and NDC subjects, were informed and consented following the principles set out in the World Medical Association Declaration of Helsinki and the Department of Health and Human Services Belmont Report, and study no. 2001P001379. Demographics for the different subject groups are listed in Table 1.

Isolation of human $CD4^+$ T cells and phenotyping via flow cytometry

Human primary $CD4^+$ T cells were isolated using the EasySep Direct Human $CD4^+$ T Cell Isolation Kit (STEMCELL Technologies, Cambridge, MA) following the manufacturer's protocol. Briefly, 1000 μl of Isolation Cocktail and 1000 μl of RapidSpheres were mixed with 20 ml of whole blood in a 50-ml centrifuge tube and incubated for 5 min at room temperature. Thirty milliliters of phosphate-buffered saline (PBS) was added, and the tube was placed into a "Easy 50" magnet (STEMCELL Technologies). This immobilized the unwanted non-$CD4^+$ T cells at the side of the tube. After 10 min, the $CD4^+$ T cell–enriched suspension was transferred into a new tube, fresh RapidSpheres were added and incubated for 5 min, and the magnetic separation was repeated. The resulting highly enriched $CD4^+$ T cell suspension was transferred into a new tube again and purified for a third time using the magnet. The final $CD4^+$ T cell preparations had purities of >95%.

For phenotyping, the isolated $CD4^+$ T cells were immediately stained with mouse allophycocyanin (APC)–labeled anti-human CD3 antibody (BioLegend, San Diego, CA) or TCRαβ antibody (BioLegend). The cells were analyzed using BD FACSCanto II (BD Biosciences, Franklin Lakes, NJ). For culture experiments with BCG, the leftover $CD4^+$ T cells were seeded in 24-well tissue culture plates at 5×10^5 cells in 1 ml of RPMI 1640 medium (Thermo Fisher Scientific, Waltham, MA) supplemented with 10% fetal bovine serum (Thermo Fisher Scientific), penicillin (100 U/ml), streptomycin (100 mg/ml; Thermo Fisher Scientific), human interleukin-2 (IL-2; 100 U/ml; MilliporeSigma, Burlington, MA), and concanavalin A (2.5 μg/ml; Thermo Fisher Scientific). BCG [1×10^5 colony-forming units (CFU); strain BCG Japan, BCG Laboratory, Tokyo, Japan] was added to half of the wells, and the other wells remained as controls. Culture was at 37°C in 5% CO_2 and 95% air. At days 3 and 5, the cells were split with the same dosage of any reagents. At day 7, the cells were harvested and washed with PBS (Thermo Fisher Scientific), then incubated with the same antibodies as above, and analyzed by flow cytometry. MFI was determined using FlowJo software (BD Biosciences).

ELISA for detecting CD3 and TCR protein

CD3 and TCR protein levels were evaluated by ELISA. Freshly isolated primary $CD4^+$ T cells were lysed by repeated freeze-thaw cycles in lysis buffer [PBS supplemented with a protein inhibitor cocktail tablet (cOmplete ULTRA Tablets, Mini, EDTA-free, EASYpack; Sigma-Aldrich, St. Louis, MO)] at 1×10^6 cells/100 μl. For in vitro culture evaluation of BCG responses, some of the isolated $CD4^+$ T cells were seeded in 24-well tissue culture plates at 1×10^6 cells in 1 ml of RPMI culture medium supplemented with 2.5% ImmunoCult Human CD3/CD28 T Cell Activator (STEMCELL Technologies) and human IL-2 (100 U/ml). BCG (1×10^5 CFU; strain BCG Japan) was added to half of the wells, and the other wells remained as controls. Culture was at 37°C in 5% CO_2 and 95% air. After 3 days of incubation, the cells were harvested and lysed by repeated freeze-thaw cycles in lysis buffer at 1×10^6 cells/100 μl. The lysate was then centrifuged at 8000*g* for 30 min, and the supernatant was tested for the presence of CD3 using Human CD3 gamma, CD3 delta, or CD3 epsilon ELISA Kits (Novus Biologicals, Centennial, CO). The levels of CD3ζ (CD247) and TCR were also measured using CD247 ELISA kits (Aviva Systems Biology, San Diego, CA) or QuickDetect TCR (Human) ELISA Kit (BioVision Inc., Milpitas, CA), respectively. Whole protein levels were measured with a BCA protein assay (Thermo Fisher Scientific), and the values were expressed as the TCR or CD3 levels (nanograms per milliliter) normalized by whole protein levels (micrograms per milliliter).

Methylation data analysis

DNA was prepared from $CD4^+$ T cells using DNeasy Blood & Tissue Kits (QIAGEN, Hilden, Germany) and stored at −80°C. For each sample, 1 μg of DNA was bisulfite-converted using the EZ-96 DNA

Methylation Kit (Shallow Well Format; Zymo Research Corporation, Irvine, CA) following the manufacturer's protocol. Standard polymerase chain reaction (PCR) of the highly methylated P19 gene was performed to confirm the quality of bisulfite conversion using primers that target known sites of methylation. The primers for the methylated targets are as follows: Bisulfite_QC.F, CTAAAACCCCA-ACTACCTAAA; Bisulfite_QC.R, TAGGTTTTTTAGGAAGGA-GAG. PCR cycling conditions were 95°C for 15 min, 5 cycles of (95°C for 30 s, 60°C for 2 min, and 72°C for 1 min), 30 cycles of (95°C for 30 s, 65°C for 1 min, and 72°C for 1 min), and 72°C for 5 min. PCR products were run on a 2% agarose gel, and a single band at 286 base pairs indicated successful conversion.

The methylation assay was performed with the Human MethylationEPIC BeadChip (Illumina, San Diego, CA) using 200 to 400 ng of bisulfite-converted DNA product for each sample according to the Infinium HD Methylation Assay protocol (Illumina). This assay targets over 850,000 known and potential methylation sites across the genome via 50-mer probes attached to the Infinium BeadChips. The bisulfite-converted DNA was hybridized to the probes on the BeadChip followed by a single base extension to incorporate a Cy3- or Cy5-labeled nucleotide at the target position to differentiate methylation status. The BeadChips were then imaged on the Illumina iScan reader, and the methylation level of each CpG locus was calculated in the GenomeStudio Methylation module as β value [intensity of the methylated allele (M)/(intensity of the unmethylated allele (U) + intensity of the methylated allele (M) + 100)]. The β values of all represented CpG sites on the chip were averaged for each gene, and the methylation patterns were then compared and displayed as the difference between NDC and T1D at baseline or as the difference of T1D at baseline versus 1 to 3 years after BCG vaccination. For TCR regional data analysis (i.e., methylation patterns in the C, V, J, and D regions), the average β values for CpGs across each segmental gene were calculated. For picking up the most hyper/hypomethylated genes, the average difference or change in β value for each CpG site of the genes was calculated, and the genes were sorted in order excluding noncoding DNA or RNA genes.

As described above, we calculated the overall methylation state of a gene at a given time point by first calculating the difference in β value of each CpG at that time point versus baseline and then by calculating an overall difference by averaging. Here, we refer to a gene as being hypermethylated if this overall β value difference is positive. For a hypomethylated or demethylated gene, this overall difference is negative.

Protein array

A protein array was performed to evaluate multiple kinase activities with the Human Phospho-Kinase Array Kit (R&D Systems, Minneapolis, MN) following the manufacturer's protocol. Samples were established by the attached lysis buffer supplemented with aprotinin, leupeptin, and pepstatin (10 μg/ml; R&D Systems). The images were developed with HYBLOT CL-Film (Thomas Scientific). The signaling strength was quantified by densitometry using ImageJ software (National Institutes of Health), and the values are expressed as relative mean pixel density against the average of those of reference spots.

mRNA sequencing data analysis

Total RNA was extracted from isolated $CD4^+$ T cells using the RNeasy Plus Mini Kit (QIAGEN). RNA-seq was performed at the Center for Cancer Computational Biology (CCCB) of the Dana-Farber Cancer Institute (DFCI) as well as at the BioMicro Center (BMC) of the Massachusetts Institute of Technology. For mRNA isolation from total RNA, NEBNext Poly(A) mRNA Magnetic Isolation Modules were used, and for library preparation, the NEBNext Ultra or NEBNext Ultra II Directional RNA Library Prep Kits for Illumina were used. Sequencing was performed with Illumina NextSeq 500 at the CCCB or with NovaSeq 6000 with S4 Flowcell at the BMC. Reads were aligned to the GRCh38.95 reference genome using the STAR Aligner application. The quality control software included FastQC, RSeQC, and MultiQC, and the reads were normalized using DESeq2.

Before the analyses, all raw data were normalized by average value in the mRNA expressions of multiple housekeeping genes including *ATCB*, *GAPDH*, *PGK1*, *YWHAZ*, *SDHA*, *TFRC*, *GUSB*, *HMBS*, and *TUBB* for the calibration among sequences. Then, the normalized mRNA value was compared and displayed as the percent change between NDC and T1D at baseline or as T1D at baseline and 1 to 3 years after BCG vaccinations. For the TCR segmental data analysis (i.e., mRNA expressions in the *CVJ* regions), the average mRNA expression at each segmental gene was used for the comparisons.

Quantitative analysis in TCRα and TCRβ

gDNA was extracted from $CD4^+$ T cells with QIAamp DNA mini kits (QIAGEN), and 128 to 430 ng of them were submitted for immunosequencing of the CDR3 regions of human TCRα/β chains using the immunoSEQ Assay (Adaptive Biotechnologies, Seattle, WA). Extracted gDNA was amplified in a bias-controlled multiplex PCR, followed by high-throughput sequencing. Sequences were collapsed and filtered to identify and quantitate the absolute abundance of each unique TCRα/β CDR3 regions for further analysis as previously described (*65*–*69*).

Statistical analyses of TCRαβ sequencing results

All data were statistically assessed by two-way analysis of variance, followed by Wilcoxon testing to compare two groups. The data of clonality and usage in TCRα and TCRβ were analyzed by paired Wilcoxon test. *P* values less than 0.05 were considered statistically significant.

Two quantitative components of diversity were compared across samples in this study. Simpson clonality was calculated on productive rearrangements by $\sqrt{\sum_{i=1}^{R} p_i^2}$, where R is the total number of rearrangements and p_i is the productive frequency of rearrangement i. Values of Simpson clonality range from 0 to 1 and measure how evenly receptor sequences (rearrangements) are distributed among a set of T cells. Clonality values approaching 0 indicate a very even distribution of frequencies, whereas values approaching 1 indicate an increasingly asymmetric distribution in which a few clones are present at higher frequencies.

Sample richness was calculated as the number of unique productive rearrangements in a sample after computationally downsampling to a common number of T cells to control for variation in sample depth. Repertoires were randomly sampled without replacement five times, and richness is reported as the mean number of unique rearrangements (downsampled to 53,679 and 7,340 templates in TCRα/β, respectively).

To calculate the number of expanded clones in each patient, rearrangement frequencies from baseline and postvaccination samples (year 2 or year 3) were compared using a binomial distribution framework as previously described (*69*). In brief, for each clone, we

performed a two-sided test that the baseline and postvaccination frequencies at year 2 or year 3 were the same. The Benjamini-Hochberg procedure was used to control FDR at 0.01 (*70*).

Diversity metrics were compared between years using Wilcoxon signed-rank tests. All statistical analyses were performed in R version 3.6.1.

Statistical analysis for methylation and RNA-seq data

Some of the methylation and RNA-seq data were not normally distributed and thus not suitable for Student's *t* testing. For consistency, we therefore calculated nonparametric statistics for these data, whether it was normally distributed or not. For unpaired data, we used Mann-Whitney *U* testing, whereas for paired data we used Wilcoxon testing. All testing was one-tailed because we had clear expectations in which direction the data would change based on previous results. FDR corrections were determined by calculating *q* values for all *P* values using the R Bioconductor qvalue package version 2.22.0. Results were only considered significant if both $P < 0.05$ and $q < 0.05$. There are hundreds of genes listed here, so to prevent clutter we have only highlighted some of the most important statistics in the text. In the figures, we indicated significant results with asterisks: $*P < 0.05$ and $q < 0.05$; $**P < 0.01$ and $q < 0.05$; $***P < 0.001$ and $q < 0.05$. A comprehensive list of all *P* and *q* values is provided in tables S1 to S4. Statistical analysis was performed in GraphPad Prism version 9.2.0 and in R version 4.0.3.

SUPPLEMENTARY MATERIALS

Supplementary material for this article is available at https://science.org/doi/10.1126/sciadv.abq7240

View/request a protocol for this paper from *Bio-protocol*.

REFERENCES AND NOTES

1. P. Aaby, A. Roth, H. Ravn, B. M. Napirna, A. Rodrigues, I. M. Lisse, L. Stensballe, B. R. Diness, K. R. Lausch, N. Lund, S. Biering-Sørensen, H. Whittle, C. S. Benn, Randomized trial of BCG vaccination at birth to low-birth-weight children: Beneficial nonspecific effects in the neonatal period? *J. Infect. Dis.* **204**, 245–252 (2011).
2. E. Elguero, K. B. Simondon, J. Vaugelade, A. Marra, F. Simondon, Non-specific effects of vaccination on child survival? A prospective study in Senegal. *Trop. Med. Int. Health* **10**, 956–960 (2005).
3. I. Kristensen, P. Aaby, H. Jensen, Routine vaccinations and child survival: Follow up study in Guinea-Bissau, West Africa. *BMJ* **321**, 1435–1438 (2000).
4. V. Nankabirwa, J. K. Tumwine, P. M. Mugaba, T. Tylleskar, H. Sommerfelt; PROMISE- EBF Study Group, Child survival and BCG vaccination: A community based prospective cohort study in Uganda. *BMC Public Health* **15**, 175 (2015).
5. M.-G. Hollm-Delgado, E. A. Stuart, R. E. Black, Acute lower respiratory infection among Bacille Calmette-Guérin (BCG)-vaccinated children. *Pediatrics* **133**, e73–e81 (2014).
6. M. J. de Castro, J. Pardo-Seco, F. Martinon-Tórres, Nonspecific (Heterologous) protection of neonatal BCG vaccination against hospitalization due to respiratory infection and sepsis. *Clin. Infect. Dis.* **60**, 1611–1619 (2015).
7. G. Ristori, M. G. Buzzi, U. Sabatini, E. Giugni, S. Bastianello, F. Viselli, C. Buttinelli, S. Ruggieri, C. Colonnese, C. Pozzilli, M. Salvetti, Use of bacille calmette-guerin (BCG) in multiple sclerosis. *Neurology* **53**, 1588–1589 (1999).
8. A. Paolillo, M. G. Buzzi, E. Giugni, U. Sabatini, S. Bastianello, C. Pozzilli, M. Salvetti, G. Ristori, The effect of Bacille Calmette-Guerin on the evolution of new enhancing lesions to hypointense T1 lesions in relapsing remitting MS. *J. Neurol.* **250**, 247–248 (2003).
9. G. Ristori, S. Romano, S. Cannoni, A. Visconti, E. Tinelli, L. Mendozzi, P. Cecconi, R. Lanzillo, M. Quarantelli, C. Buttinelli, C. Gasperini, M. Frontoni, G. Coarelli, D. Caputo, V. Bresciamorra, N. Vanacore, C. Pozzilli, M. Salvetti, Effects of Bacille Calmette-Guerin after the first demyelinating event in the CNS. *Neurology* **82**, 41–48 (2014).
10. D. L. Faustman, L. Wang, Y. Okubo, D. Burger, L. Ban, G. Man, H. Zheng, D. Schoenfeld, R. Pompei, J. Avruch, D. M. Nathan, Proof-of-concept, randomized, controlled clinical trial of Bacillus-Calmette-Guerin for treatment of long-term type 1 diabetes. *PLOS ONE* **7**, e41756 (2012).
11. W. M. Kuhtreiber, D. L. Faustman, BCG therapy for type 1 diabetes: Restoration of balanced immunity and metabolism. *Trends Endocrinol. Metab.* **30**, 80–92 (2019).
12. W. M. Kühtreiber, L. Tran, T. Kim, M. Dybala, B. Nguyen, S. Plager, D. Huang, S. Janes, A. Defusco, D. Baum, H. Zheng, D. L. Faustman, Long-term reduction in hyperglycemia in advanced type 1 diabetes: The value of induced aerobic glycolysis with BCG vaccinations. *NPJ Vaccines* **3**, 23 (2018).
13. W. M. Kühtreiber, H. Takahashi, R. C. Keefe, Y. Song, L. Tran, T. G. Luck, G. Shpilsky, L. Moore, S. M. Sinton, J. C. Graham, D. L. Faustman, BCG Vaccinations upregulate myc, a central switch for improved glucose metabolism in diabetes. *iScience* **23**, 101085 (2020).
14. S. Guallar-Garrido, E. Julián, Bacillus Calmette-Guérin (BCG) therapy for bladder cancer: An update. *Immunotargets Ther.* **9**, 1–11 (2020).
15. N. T. Usher, S. Chang, R. S. Howard, A. Martinez, L. H. Harrison, M. Santosham, N. E. Aronson, Association of BCG vaccination in childhood with subsequent cancer diagnoses: A 60-year follow-up of a clinical trial. *JAMA Netw. Open* **2**, e1912014 (2019).
16. M. K. Lalor, S. G. Smith, S. Floyd, P. Gorak-Stolinska, R. E. Weir, R. Blitz, K. Branson, P. E. Fine, H. M. Dockrell, Complex cytokine profiles induced by BCG vaccination in UK infants. *Vaccine* **28**, 1635–1641 (2010).
17. J. Sharrock, J. C. Sun, Innate immunological memory: From plants to animals. *Curr. Opin. Immunol.* **62**, 69–78 (2020).
18. D. M. E. Bowdish, M. S. Loffredo, S. Mukhopadhyay, A. Mantovani, S. Gordon, Macrophage receptors implicated in the "adaptive" form of innate immunity. *Microbes Infect.* **9**, 1680–1687 (2007).
19. M. G. Netea, L. A. Joosten, E. Latz, K. H. Mills, G. Natoli, H. G. Stunnenberg, L. A. O'Neill, R. J. Xavier, Trained immunity: A program of innate immune memory in health and disease. *Science* **352**, aaf1098 (2016).
20. V. R. Ramirez-Carrozzi, D. Braas, D. M. Bhatt, C. S. Cheng, C. Hong, K. R. Doty, J. C. Black, A. Hoffmann, M. Carey, S. T. Smale, A unifying model for the selective regulation of inducible transcription by CpG islands and nucleosome remodeling. *Cell* **138**, 114–128 (2009).
21. J. Kleinnijenhuis, J. Quintin, F. Preijers, C. S. Benn, L. A. Joosten, C. Jacobs, J. van Loenhout, R. J. Xavier, P. Aaby, J. W. van der Meer, R. van Crevel, M. G. Netea, Long-lasting effects of BCG vaccination on both heterologous Th1/Th17 responses and innate trained immunity. *J. Innate Immun.* **6**, 152–158 (2014).
22. J. Madura Larsen, C. S. Benn, Y. Fillie, D. van der Kleij, P. Aaby, M. Yazdanbakhsh, BCG stimulated dendritic cells induce an interleukin-10 producing T-cell population with no T helper 1 or T helper 2 bias in vitro. *Immunology* **121**, 276–282 (2007).
23. M. E. Call, K. W. Wucherpfennig, The T cell receptor: Critical role of the membrane environment in receptor assembly and function. *Annu. Rev. Immunol.* **23**, 101–125 (2005).
24. E. Hodges, M. T. Krishna, C. Pickard, J. L. Smith, Diagnostic role of tests for T cell receptor (TCR) genes. *J. Clin. Pathol.* **56**, 1–11 (2003).
25. F. W. Alt, E. M. Oltz, F. Young, J. Gorman, G. Taccioli, J. Chen, VDJ recombination. *Immunol. Today* **13**, 306–314 (1992).
26. B. Alarcon, D. Gil, P. Delgado, W. W. Schamel, Initiation of TCR signaling: Regulation within CD3 dimers. *Immunol. Rev.* **191**, 38–46 (2003).
27. L. D. Notarangelo, Immunodeficiency and immune dysregulation associated with proximal defects of T cell receptor signaling. *Curr. Opin. Immunol.* **31**, 97–101 (2014).
28. A. G. Schrum, L. A. Turka, E. Palmer, Surface T-cell antigen receptor expression and availability for long-term antigenic signaling. *Immunol. Rev.* **196**, 7–24 (2003).
29. H. K. Dadi, A. J. Simon, C. M. Roifman, Effect of CD3δ deficiency on maturation of α/β and γ/δ T-cell lineages in severe combined immunodeficiency. *N. Engl. J. Med.* **349**, 1821–1828 (2003).
30. G. de Saint Basile, F. Geissmann, E. Flori, B. Uring-Lambert, C. Soudais, M. Cavazzana-Calvo, A. Durandy, N. Jabado, A. Fischer, F. Le Deist, Severe combined immunodeficiency caused by deficiency in either the delta or the epsilon subunit of CD3. *J. Clin. Invest.* **114**, 1512–1517 (2004).
31. N. V. Morgan, S. Goddard, T. S. Cardno, D. McDonald, F. Rahman, D. Barge, A. Ciupek, A. Straatman-Iwanowska, S. Pasha, M. Guckian, G. Anderson, A. Huissoon, A. Cant, W. P. Tate, S. Hambleton, E. R. Maher, Mutation in the TCRalpha subunit constant gene (TRAC) leads to a human immunodeficiency disorder characterized by a lack of TCRalphabeta$^+$ T cells. *J. Clin. Invest.* **121**, 695–702 (2011).
32. D. Faustman, D. Schoenfeld, R. Ziegler, T-lymphocyte changes linked to autoantibodies: Association of insulin autoantibodies with CD4$^+$CD45R$^+$ lymphocyte subpopulation in prediabetic subjects. *Diabetes* **40**, 590–597 (1991).
33. D. Faustman, G. Eisenbarth, J. Daley, J. Breitmeyer, Abnormal T lymphocyte subsets in type I diabetes mellitus: Analysis with anti-2H4 and anti-4B4 antibodies. *Diabetes* **38**, 1462–1468 (1989).
34. D. L. Faustman, Occult CD45 T cell developmental defect in type I diabetes. *Diabetes Metab.* **19**, 446–457 (1993).
35. D. A. Mendes-da-Cruz, J. P. Lemos, G. A. Passos, W. Savino, Abnormal T-cell development in the thymus of non-obese diabetic mice: Possible relationship with the pathogenesis of type 1 autoimmune diabetes. *Front. Endocrinol. (Lausanne)* **9**, 381 (2018).

36. S. Bannister, N. L. Messina, B. Novakovic, N. Curtis, The emerging role of epigenetics in the immune response to vaccination and infection: A systematic review. *Epigenetics* **15**, 555–593 (2020).
37. L. Riber, L. H. Hansen, Epigenetic memories: The hidden drivers of bacterial persistence? *Trends Microbiol.* **29**, 190–194 (2021).
38. S. B. Rothbart, B. D. Strahl, Interpreting the language of histone and DNA modifications. *Biochim. Biophys. Acta* **1839**, 627–643 (2014).
39. J. Kleinnijenhuis, J. Quintin, F. Preijers, L. A. Joosten, D. C. Ifrim, S. Saeed, C. Jacobs, J. van Loenhout, D. de Jong, H. G. Stunnenberg, R. J. Xavier, J. W. van der Meer, R. van Crevel, M. G. Netea, Bacille Calmette-Guerin induces NOD2-dependent nonspecific protection from reinfection via epigenetic reprogramming of monocytes. *Proc. Natl. Acad. Sci. U.S.A.* **109**, 17537–17542 (2012).
40. R. J. W. Arts, S. Moorlag, B. Novakovic, Y. Li, S. Y. Wang, M. Oosting, V. Kumar, R. J. Xavier, C. Wijmenga, L. A. B. Joosten, C. Reusken, C. S. Benn, P. Aaby, M. P. Koopmans, H. G. Stunnenberg, R. van Crevel, M. G. Netea, BCG vaccination protects against experimental viral infection in humans through the induction of cytokines associated with trained immunity. *Cell Host Microbe* **23**, 89–100.e5 (2018).
41. D. P. Strachan, Hay fever, hygiene, and household size. *Br. Med. J.* **299**, 1259–1260 (1989).
42. K. Hirahara, G. Vahedi, K. Ghoreschi, X. P. Yang, S. Nakayamada, Y. Kanno, J. J. O'Shea, A. Laurence, Helper T-cell differentiation and plasticity: Insights from epigenetics. *Immunology* **134**, 235–245 (2011).
43. J. H. Rowe, O. M. Delmonte, S. Keles, B. D. Stadinski, A. K. Dobbs, L. A. Henderson, Y. Yamazaki, L. M. Allende, F. A. Bonilla, L. I. Gonzalez-Granado, S. Celikbilek Celik, S. N. Guner, H. Kapakli, C. Yee, S. Y. Pai, E. S. Huseby, I. Reisli, J. R. Regueiro, L. D. Notarangelo, Patients with *CD3G* mutations reveal a role for human CD3γ in T_{reg} diversity and suppressive function. *Blood* **131**, 2335–2344 (2018).
44. J. R. Cochran, T. O. Cameron, J. D. Stone, J. B. Lubetsky, L. J. Stern, Receptor proximity, not intermolecular orientation, is critical for triggering T-cell activation. *J. Biol. Chem.* **276**, 28068–28074 (2001).
45. H. Cai, J. Muller, D. Depoil, V. Mayya, M. P. Sheetz, M. L. Dustin, S. J. Wind, Full control of ligand positioning reveals spatial thresholds for T cell receptor triggering. *Nat. Nanotechnol.* **13**, 610–617 (2018).
46. N. R. Gascoigne, V. Rybakin, O. Acuto, J. Brzostek, TCR signal strength and T cell development. *Annu. Rev. Cell Dev. Biol.* **32**, 327–348 (2016).
47. G. Gaud, R. Lesourne, P. E. Love, Regulatory mechanisms in T cell receptor signalling. *Nat. Rev. Immunol.* **18**, 485–497 (2018).
48. S. Tanaka, S. Maeda, M. Hashimoto, C. Fujimori, Y. Ito, S. Teradaira, K. Hirota, H. Yoshitomi, T. Katakai, A. Shimizu, T. Nomura, N. Sakaguchi, S. Sakaguchi, Graded attenuation of TCR signaling elicits distinct autoimmune diseases by altering thymic T cell selection and regulatory T cell function. *J. Immunol.* **185**, 2295–2305 (2010).
49. L. Conti, M. Cardone, B. Varano, P. Puddu, F. Belardelli, S. Gessani, Role of the cytokine environment and cytokine receptor expression on the generation of functionally distinct dendritic cells from human monocytes. *Eur. J. Immunol.* **38**, 750–762 (2008).
50. S. Booy, C. H. van Eijck, F. Dogan, P. M. van Koetsveld, L. J. Hofland, Influence of type-I Interferon receptor expression level on the response to type-I interferons in human pancreatic cancer cells. *J. Cell. Mol. Med.* **18**, 492–502 (2014).
51. M. B. Lutz, M. Schnare, M. Menges, S. Rossner, M. Rollinghoff, G. Schuler, A. Gessner, Differential functions of IL-4 receptor types I and II for dendritic cell maturation and IL-12 production and their dependency on GM-CSF. *J. Immunol.* **169**, 3574–3580 (2002).
52. W. Jiang, V. M. Estes, X. S. Wang, Z. Shao, B. J. Lee, X. Lin, J. L. Crowe, S. Zha, Phosphorylation at S2053 in murine (S2056 in Human) DNA-PKcs is dispensable for lymphocyte development and class switch recombination. *J. Immunol.* **203**, 178–187 (2019).
53. B. Alarcon, M. Swamy, H. M. van Santen, W. W. Schamel, T-cell antigen-receptor stoichiometry: Pre-clustering for sensitivity. *EMBO Rep.* **7**, 490–495 (2006).
54. S. T. Jerram, M. N. Dang, R. D. Leslie, The role of epigenetics in type 1 diabetes. *Curr. Diab. Rep.* **17**, 89 (2017).
55. B. A. Schodin, T. J. Tsomides, D. M. Kranz, Correlation between the number of T cell receptors required for T cell activation and TCR-ligand affinity. *Immunity* **5**, 137–146 (1996).
56. R. A. Gottschalk, E. Corse, J. P. Allison, TCR ligand density and affinity determine peripheral induction of Foxp3 in vivo. *J. Exp. Med.* **207**, 1701–1711 (2010).
57. C. Joseph, J. Klibi, L. Amable, L. Comba, A. Cascioferro, M. Delord, V. Parietti, C. Lenoir, S. Latour, B. Lucas, C. Viret, A. Toubert, K. Benlagha, TCR density in early iNKT cell precursors regulates agonist selection and subset differentiation in mice. *Eur. J. Immunol.* **49**, 894–910 (2019).
58. Y. Okubo, H. Torrey, J. Butterworth, H. Zheng, D. L. Faustman, Treg activation defect in type 1 diabetes: Correction with TNFR2 agonism. *Clin. Transl. Immunol.* **5**, e56 (2016).
59. R. C. Keefe, H. Takahashi, L. Tran, K. Nelson, N. Ng, W. M. Kuhtreiber, D. L. Faustman, BCG therapy is associated with long-term, durable induction of Treg signature genes by epigenetic modulation. *Sci. Rep.* **11**, 14933 (2021).
60. R. Huang, J. Guo, X. Li, D. L. Faustman, Elimination of self-peptide major histocompatibility complex class I reactivity in NOD and ß2-microglobulin-negative mice. *Diabetes* **44**, 1114–1120 (1995).
61. F. Li, J. Guo, Y. Fu, G. Yan, D. Faustman, Abnormal class I assembly and peptide presentation in the diabetic NOD mouse. *Proc. Natl. Acad. Sci. U.S.A.* **91**, 11128–11132 (1994).
62. D. Faustman, X. Li, H. Y. Lin, Y. Fu, G. Eisenbarth, J. Avruch, J. Guo, Linkage of faulty major histocompatibility complex class I to autoimmune diabetes. *Science* **254**, 1756–1761 (1991).
63. Y. Fu, D. M. Nathan, F. Li, X. Li, D. L. Faustman, Defective major histocompatibility complex class I expression on lymphoid cells in autoimmunity. *J. Clin. Invest.* **91**, 2301–2307 (1993).
64. R. Mazzone, C. Zwergel, M. Artico, S. Taurone, M. Ralli, A. Greco, A. Mai, The emerging role of epigenetics in human autoimmune disorders. *Clin. Epigenetics* **11**, 34 (2019).
65. H. S. Robins, P. V. Campregher, S. K. Srivastava, A. Wacher, C. J. Turtle, O. Kahsai, S. R. Riddell, E. H. Warren, C. S. Carlson, Comprehensive assessment of T-cell receptor beta-chain diversity in alphabeta T cells. *Blood* **114**, 4099–4107 (2009).
66. C. S. Carlson, R. O. Emerson, A. M. Sherwood, C. Desmarais, M. W. Chung, J. M. Parsons, M. S. Steen, M. A. LaMadrid-Herrmannsfeldt, D. W. Williamson, R. J. Livingston, D. Wu, B. L. Wood, M. J. Rieder, H. Robins, Using synthetic templates to design an unbiased multiplex PCR assay. *Nat. Commun.* **4**, 2680 (2013).
67. N. Ritz, B. Dutta, S. Donath, D. Casalaz, T. G. Connell, M. Tebruegge, R. Robins-Browne, W. A. Hanekom, W. J. Britton, N. Curtis, The influence of bacille Calmette-Guerin vaccine strain on the immune response against tuberculosis: A randomized trial. *Am. J. Respir. Crit. Care Med.* **185**, 213–222 (2012).
68. H. Robins, C. Desmarais, J. Matthis, R. Livingston, J. Andriesen, H. Reijonen, C. Carlson, G. Nepom, C. Yee, K. Cerosaletti, Ultra-sensitive detection of rare T cell clones. *J. Immunol. Methods* **375**, 14–19 (2012).
69. W. S. DeWitt, R. O. Emerson, P. Lindau, M. Vignali, T. M. Snyder, C. Desmarais, C. Sanders, H. Utsugi, E. H. Warren, J. McElrath, K. W. Makar, A. Wald, H. S. Robins, Dynamics of the cytotoxic T cell response to a model of acute viral infection. *J. Virol.* **89**, 4517–4526 (2015).
70. Y. Benjamini, J. Hochberg, Controlling the false discovery rate: A practical and powerful approach to multiple testing. *J. R. Stat. Soc. Ser. B Methodol.* **57**, 289–300 (1995).

Acknowledgments: We thank L. Murphy and S. A. Williams for administrative support. We thank M. Davis for detailed proofreading of the paper. We also thank M. Vignali for editing of the final paper. **Funding:** This work was funded by all nonprofit foundation gifts to the laboratory.
Author contributions: Conceptualization: R.C.K., H.T., W.M.K., and D.L.F. Methodology: H.T., W.M.K., R.C.K., H.F.D., D.L.F., S.B., and D.S. Investigation: H.T., W.M.K., R.C.K., A.H.L., S.B., D.S., A.A., N.N., and K.J.N. Writing: H.T., W.M.K., and D.L.F. Supervision: W.M.K. and D.L.F.
Competing interests: S.B. has a financial interest in Adaptive Biotechnologies. The authors declare no other competing interests. **Data and materials availability:** All data needed to evaluate the conclusions in the paper are present in the paper and/or the Supplementary Materials.

Submitted 26 April 2022
Accepted 27 September 2022
Published 16 November 2022
10.1126/sciadv.abq7240